Furthermore, the relationship between changes in normal-range BP and cognitive function—particularly the implications of lower BP—remains to be clarified. In fact, there have been few studies directly exploring the effect of low BP on cognitive function. Guo *et al.* (*3*) have reported that low-level BP is related to an impairment of cognition. On the other hand, J-curve (*4*) or U-shaped (*5*) relationships between BP values and performance on cognitive tests have also been reported. However, the subjects in these studies were elderly, mostly over 75 years old, and included patients who had suffered from hypertension for a long period. In such subjects, BP reduction is likely to cause cerebrovascular hypoperfusion through a resetting of hemodynamic autoregulation. Moreover, it has also been reported that cerebrovascular diseases or dementia underlying cognitive impairment lowers BP *per se*, thereby producing a further deterioration of cognitive function (*6*, *7*). Thus the elderly cohorts used in previous studies have tended to complicate the interpretation of the relationship between BP and cognitive function. Hence, to explore the possible effect of lower levels of BP on cognitive function, younger and healthier subjects who are less likely to have suffered from cerebrovascular damage should be analyzed. Accordingly, we here used a cohort of normotensive, middle-aged women to explore the effects of lower levels of BP on cognitive function.

Subjects and Methods

Subjects

Among post-menopausal women who visited our Health Service Center for medical check-ups, 26 women aged 56 to 60 years old were recruited randomly for participation in the present study. All the subjects were well informed of the objective and outlines of the tests and gave their informed consent to participate in this project. Systolic blood pressure (SBP) and diastolic blood pressure (DBP) were measured 3 times at 1-month intervals by a well-trained registered nurse. At each visit for BP determination, BP was measured 3 times at 5-min intervals in the morning with subjects in a seated position after 30-min of relaxation in a quiet room, and then was measured. The criteria for normotension were <140 mmHg for SBP and <90 mmHg for DBP according to the classification recommended by 1999 WHO/ISH (*8*). Twenty-two subjects were diagnosed as normotensive because their BP values were all within the normal range throughout the evaluation period. Four subjects were hypertensive, including 1 subject who was taking anti-hypertensive drugs. These 4 cases were excluded, and the remaining 22 subjects were analyzed in this study. None of the subjects had a history of stroke or any signs/symptoms suggestive of established dementia or disorders of the central nervous system. None of the subjects were taking medicines that would affect cognitive function.

Physical Measurements

All measurements of SBP and DBP of each subject were averaged respectively, and the values were used for the following analyses. At the last visit for BP evaluation, heart rate (HR), body weight, and height were also measured using standard electrical devices. Body mass index (BMI) was defined as body weight (kg) / (height (m))^2. In addition, blood samples were obtained to determine serum concentrations of total cholesterol (TC) and fasting blood glucose (FBS).

Psychometric Assessments

After measuring physical characteristics, psychometric tests, including Wechsler Adult Intelligence Scale-Revised (WAIS-R) subtests, were administered by a designated specialist for psychological examination. The examiner was blinded to all patient characteristics. Standardized procedures from published manuals were used in the test administration and evaluation. Cognitive function was measured using WAIS-R subtests (*9*), which are widely used instruments for evaluating intelligence in adults. Because it takes so long time to perform a full set of WAIS-R subtests, eight subtests were selected and administered in the present study: 1) Information, 2) Digit Span, 3) Similarities, 4) Picture Completion, 5) Picture Arrangement, 6) Block Design, 7) Object Assembly, and 8) Digit Symbol. The Digit Symbol Test largely reflects psychomotor speed and is independent of influences from the other factors (*10*). Scores for each subtest were expressed as the percentage of correct responses. The Yatabe-Guilford (Y-G) test (*11*), which is a self-reported, multiple-choice questionnaire, was used to evaluate the character traits of the subjects.

Educational Level

Educational level was expressed as the total length of education: *i.e.*, 6 years for elementary school, 3 years for junior high school, 3 years for senior high school, 2 years for technical college, 2 years for junior college, 4 years for university, and 2 years for graduate school.

Statistical Analysis

Statistical analyses were performed using STATISTICA software (StatSoft, Tulsa, USA) on a computer running the Windows operating system. To test the possible relationship between cognitive tests and BP, both simple correlations and partial correlations controlling for the effects of other variables were examined. Stepwise multiple regression analysis was also performed to find the most important predictor variables for cognitive test scores.

Table 1. Demographic Characteristics of the Participants

Variables	Values*
Age (years)	57.7±1.1
SBP (mmHg)	120.5±10.9
DBP (mmHg)	76.1±10.1
Heart rate (beat/min)	71.7±9.2
Body mass index (kg/m^2)	21.9±2.5
Total cholesterol (mmol/l)	5.9±0.8
Fasting blood glucose (mmol/l)	6.0±1.5
Education (years)	14.7±2.1

* Values are expressed as the mean±SD.

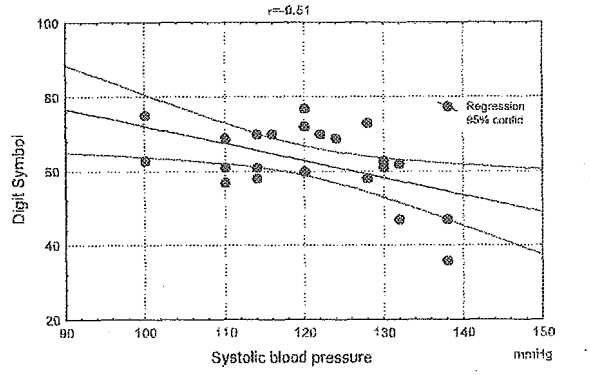

Fig. 1. *Negative correlation between Digit Symbol Test values and systolic blood pressure within normal range. A correlation was seen between Digit Symbol Test values and systolic blood pressure.*

Table 2. Cognitive Tests Scores of the Subjects

WAIS-R subtests	Score †
Information	68.5±15.2
Digit span	45.9±13.3
Similarities	61.0±16.3
Picture completion	56.1±16.9
Picture arrangement	59.3±12.7
Block design	61.1±16.7
Object assembly	64.2±10.9
Digit symbol	67.4±10.7

Scores for each subtest were expressed as the percentage of correct responses. WAIS-R, Wechsler Adult Intelligence Scale-Revised. † Values are expressed as the mean±SD.

Table 3. Correlations between BP and WAIS-R Results Adjusted by Age and Educational Level

WAIS-R subtests	Partial correlations	
	SBP	DBP
Information	−0.32	−0.33
Similarities	0.15	0.07
Picture completion	−0.27	−0.33
Picture arrangement	0.37	0.38
Block design	0.03	−0.05
Object assembly	−0.16	−0.08
Digit span	0.37	0.25
Digit symbol	−0.56*	−0.28

WAIS-R, Wechsler Adult Intelligence Scale-Revised. Partial correlations are controlled for age and educational level. *$p<0.05$.

Results

Basal Characteristics of the Subjects

The basal characteristics of the subjects are shown in Table 1. The range of SBP was 100–138 mmHg, and that of DBP was 50–88 mmHg. SBP and DBP were not related to age, BMI or HR. There was no correlation between BP level and either TC or FBS. The values of demographic characteristics exhibited a normal distribution pattern when assessed by the Shapiro-Wilk's W test (data not shown). Cognitive test scores of the subjects are shown in Table 2. The mean score of the WAIS-R subtests, excluding the Digit Symbol Test, was within the normal range for Japanese aged 55 to 64 years. The average score of the Digit Symbol Test (67.4) was slightly higher than the normal range for Japanese of this age group (30.1–61.3).

The values of risk factors shown in Table 1 and the score of cognitive tests were mostly within the normal range, and there was no polarization among these values. These data indicated that the group employed in the present study was a non-deviated, representative cohort of healthy middle-aged Japanese women.

Association of Blood Pressure with Cognitive Functions

The results clearly demonstrated that SBP was related to the Digit Symbol Test ($r=-0.51$, $p<0.05$) (Fig. 1), which principally reflects psychomotor speed. In contrast, DBP was not related to the Digit Symbol Test ($r=-0.33$, $p=0.13$) (data not shown).

Cognitive test scores are known to be influenced by age and educational attainment (*12*). In particular, age could cause a spurious negative correlation between the SBP and the Digit Symbol Test due to its positive correlation with the SBP and negative correlation with the Digit Symbol Test. To examine this possibility, we computed a partial correlation between the SBP and the Digit Symbol Test controlling for the effects of age, and obtained the value of −0.55 ($p<0.05$), which is even higher than the simple correlation reported above.

By also controlling for educational level, we could focus

Table 4. Important Predictors of the Digit Symbol Test Based on Multiple Stepwise Regression Analysis

Risk factors	β	p value
Age	−0.52	<0.05
SBP	−0.39	<0.05

Multiple correlation coefficient: $r^2=0.48$. $F=5.70$ ($p<0.05$). The dependent variable is the score on the Digit Symbol Test. Independent variables included in the multiple stepwise regression analysis are age, education, SBP, heart rate, body mass index, glucose, and total cholesterol.

on those components of the Digit Symbol Test that are unrelated to educational level. The partial correlation between the SBP and the Digit Symbol Test after controlling for age and educational level was also significant ($r=-0.56$, $p<0.05$). As shown in Table 3, no subtests of WAIS-R other than the Digit Symbol Test were related to either SBP or DBP.

Multiple Stepwise Linear Regression Analysis

Since the levels of FBS, TC and BP have been known to cluster together (*13*, *14*), stepwise multiple regression analysis was used to extract the most important predictors for the Digit Symbol Test from among the risk factors. Among the variables, which included age, education, SBP, HR, BMI, FBS, and TC, SBP and age were demonstrated to be the most potent predictors (Table 4). The other factors, including glucose and cholesterol metabolism, did not influence the cognitive function.

To assess the effect of the twelve character traits of the Y-G test, each of the traits was entered into a regression model for the Digit Symbol Test using SBP and age as independent variables. No character trait was found to make a significant contribution to the prediction (data not shown).

Discussion

In the present study, we demonstrated a negative correlation between SBP within normotensive range and the Digit Symbol Test for assessing psychomotor performance. In some previous studies, a broad range of BP levels from normotension to severe hypertension was analyzed and they found an inverse linier correlation between BP level and score of cognitive tests (*15*, *16*). These results are believed to reflect the effects of severe hypertension on cognitive function. That is, while these studies highlighted the influence of high BP *per se*, they did not isolate the role of normal-range BP. In this sense, we revealed the close association between the BP within normal range and cognitive function for the first time.

We examined cognitive function in apparently normal subjects. For this reason, any changes in cognitive function were likely to be slight. This prompted us to use the WAIS-R test to assess the decline in cognitive function, since this test is more sensitive than the standard diagnostic tools of dementia, *i.e.*, the Mini-Mental State Examination and revised version of Hasegawa's Dementia Scale. In this study, eight WAIS-R subtests were administered, with each constructed to assess a different aspect of cognitive function. Among the eight WAIS-R subtests, only the Digit Symbol Test for assessing psychomotor speed ability was correlated with SBP values. Several previous studies have reported that the effect of hypertension is the most consistent for psychomotor speed and mental status measure (*12*). On the other hand, crystallized domain, *i.e.*, information and similarities, is the most stable and resistant to BP effects (*12*, *16*). A decline in Digit Symbol Test values is also known to be associated with parietotemporal perfusion defects (*17*). Parietotemporal perfusion is regulated by branches of the internal carotid artery, and is subject to arterial injury following increases in BP. The correlation between Digit Symbol Test values and SBP within normal range may be mediated by the liability of blood perfusion in the particular blood vessels. Another possibility is that only the most powerful association is detected because of the narrow range of BP.

We demonstrated that normotensive SBP, but not DBP, is associated with reduced cognitive function. Some of the longitudinal, prospective studies have emphasized the role of higher SBP, rather than DBP, in cognitive decline in the elderly (*18–20*). In consideration of these data, we cannot overestimate the importance of midlife SBP values on eventual cognitive impairment. It was beyond the scope of the present study to clarify the mechanisms underlying the relationship between SBP and cognitive dysfunction. However, Swan *et al.* (*21*) have demonstrated that the long-term effects of SBP in midlife on deterioration of cognitive function in late-life are mediated by cerebrovascular lesions. In fact, two different groups have revealed that not only high SBP, but also moderate increase in SBP within normal range, behaves as an independent risk factor for silent lacunar infarcts (*22*, *23*). All things considered, it seems probable that a moderate increase in SBP in midlife already exerts a direct effect on cerebral vascular vessels and produces brain dysfunction.

We were unable to confirm previous reports of an association between lower BP and cognitive decline (*3–5*). Since our healthy, normotensive subjects were presumably free from cerebrovascular damage, the J-shape-like phenomenon was not found in our study.

Metabolic disturbances, especially in lipid and glucose metabolisms, are considered to be associated with cognitive function through cerebrovascular lesions. In studies from other laboratories, hyperinsulinemia, diabetes mellitus, or hypercholesterolemia have been reported to contribute to impaired cognitive function (*24*, *25*). In this study, however, we demonstrated that mild abnormalities in levels of FBS or serum TC did not influence cognitive function.

One limitation of the present study is the small sample size. However, it should be noted that a statistically significant correlation was obtained between BP and cognitive

functions regardless of the insufficient statistical power due to the small sample size, and regardless of the limited range of BP, which tends to decrease the size of correlation.

In conclusion, a moderate increase in SBP within normotensive range appears to be related to cognitive deterioration. To sustain the cognitive function, a lower SBP is ideal in normotensive, middle-aged women. In addition, a decline in Digit Symbol Test values has been reported to be a marker sensitive enough to assess progression of dementia (*26*). However, because this was an observational study, we are unable to address this point at this time. A large-scale, prospective study will be needed as a next step to confirm our present findings.

References

1. Fabrigoule C, Rouch I, Taberly A, *et al*: Cognitive process in preclinical phase of dementia. *Brain* 1998; **121**: 135–141.
2. Forette F, Seux ML, Staessen JA, *et al*: Prevention of dementia in randomised double-blind placebo-controlled Systolic Hypertension in Europe (Syst-Eur) trial. *Lancet* 1998; **352**: 1347–1351.
3. Guo Z, Viitanen M, Winblad B: Clinical correlates of low blood pressure in very old people: the importance of cognitive impairment. *J Am Geriatr Soc* 1997; **45**: 701–705.
4. Okumiya K, Matsubayashi K, Wada T, Osaki Y, Doi Y, Ozawa T: J-curve relation between blood pressure and decline in cognitive function in older people living in community, Japan. *J Am Geriatr Soc* 1997; **45**: 1032–1033.
5. Glynn RJ, Beckett LA, Hebert LE, Morris MC, Scherr PA, Evans DA: Current and remote blood pressure and cognitive decline. *JAMA* 1999; **281**: 438–445.
6. Skoog I, Lernfelt B, Landahl S, *et al*: 15-year longitudinal study of blood pressure and dementia. *Lancet* 1996; **347**:1141–1145.
7. Guo Z, Viitanen M, Fratiglioni L, Winblad B: Low blood pressure and dementia in elderly people: the Kungsholmen project. *BMJ* 1996; **312**: 805–808.
8. Guidelines Subcommittee: 1999 World Health Organization-International Society of Hypertension Guidelines for the Treatment of Hypertension. *J Hypertens* 1999; **17**: 151–183
9. Wechsler D: Wechsler Adult Intelligence Scale-Revised. New York, Psychological Corp., 1981.
10. Salthouse TA: What do adult age differences in the Digit Symbol Substitution Test reflect? *J Gerontol* 1992; **47**: 121–128.
11. Tsujioka B: New Personality Test. Tokyo, Takei-Kiki-kougyou, 1965 (in Japanese).
12. Anstey K, Christensen H: Education, activity, health, blood pressure and apolipoprotein E as predictors of cognitive change in old age: a review. *Gerontology* 2000; **46**: 163–177.
13. Kato J, Kikuya M, Matsubara M, *et al*: Risk factors and predictors of coronary arterial lesions in Japanese hypertensive patients. *Hypertens Res* 2001; **24**: 3–11.
14. Imazu M, Yamamoto H, Toyofuku M, *et al*: Hyperinsulinemia for the development of hypertension: data from the Hawaii-Los Angeles-Hiroshima Study. *Hypertens Res* 2001; **24**: 531–536.
15. Elias MF, Wolf PA, D'Agostino RB, Cobb J, White LR: Untreated blood pressure level is inversely related to cognitive functioning: the Framinghan Study. *Am J Epidemiol* 1993; **138**: 353–364.
16. Elias MF, Robbin MA, Elias PK, Streeten DHP: A longitudinal study of blood pressure in relation to performance on the Wechsler Adult Intelligence Scale. *Health Psychol* 1998; **17**: 486–493.
17. Alexander GE, Prohovnik I, Stern Y, Mayeux R: WAIS-R subtest profile and cortical perfusion in Alzheimer's disease. *Brain Cogn* 1994; **24**: 24–43.
18. Launer LJ, Masaki K, Petrovitch H, Foley D, Havlik RJ: The association between midlife blood pressure and late-life cognitive function: the Honolulu-Asia Aging Study. *JAMA* 1995; **274**: 1846–1851.
19. Starr JM, Deary IJ, Inch S, Cross S, MacLennan WJ: Blood pressure and cognitive decline in healthy old people. *J Hum Hypertens* 1997; **11**: 777–781.
20. Kanemaru A, Kanemaru K, Kuwajima I: The effects of short-term blood pressure variability and nighttime blood pressure levels on cognitive function. *Hypertens Res* 2001: **24**: 19–24.
21. Swan GE, DeCarli C, Miller BL, *et al*: Association of midlife blood pressure to late-life cognitive decline and brain morphology. *Neurology* 1998; **51**: 986–993.
22. Tanizaki Y, Kiyohara Y, Kato I, *et al*: Incidence and risk factors for subtypes of cerebral infarction in a general population: the Hisayama study. *Stroke* 2000; **31**: 2616–2622.
23. Shintani S, Shiigai T, Arinami T: Silent lacunar infarction on magnetic resonance imaging (MRI): risk factors. *J Neurol Sci* 1998; **160**: 82–86.
24. Kilander L, Nyman H, Boberg, Hansson L, Lithell H: Hypertension is related to cognitive impairment: a 20-year follow-up of 999 men. *Hypertension* 1998; **31**: 780–786.
25. Desmond DW, Tatemichi TK, Paik M, Stern Y: Risk factors for cerebrovascular disease as correlates of cognitive function in a stroke-free cohort. *Arch Neurol* 1993; **50**: 162–166.
26. Masur DM, Sliwinski M, Lipton RB, Blau AD, Crystal HA: Neuropsychological prediction of dementia and the absence of dementia in healthy elder persons. *Neurology* 1994; **44**: 1427–1432.

ELSEVIER

Cardiovascular Research 59 (2003) 419–427

Cardiovascular Research

www.elsevier.com/locate/cardiores

Decrease in sarcoglycans and dystrophin in failing heart following acute myocardial infarction

Hiroyuki Yoshida[a], Masaya Takahashi[a], Miki Koshimizu[a], Kouichi Tanonaka[a], Ryo Oikawa[a], Teruhiko Toyo-oka[b], Satoshi Takeo[a,*]

[a]*Department of Pharmacology, Tokyo University of Pharmacy and Life Science, 1432-1 Horinouchi, Hachioji, Tokyo 192-0392, Japan*
[b]*Department of Organ Pathophysiology and Internal Medicine, Tokyo University Hospital, Tokyo 113-8655, Japan*

Received 28 January 2003; received in revised form 8 March 2003; accepted 9 April 2003

Abstract

Objective: Genetic defects in several sarcoglycans (SGs) and dystrophin (Dys) play a critical role in cardiomyopathy. The present study was designed to determine whether changes in SGs and Dys might occur in animals with chronic heart failure (CHF) induced by acute myocardial infarction (AMI), which have no genetic defects. **Methods:** AMI was induced by the left coronary artery ligation (CAL) in rats. The hemodynamic parameters of the 2- and 8-week CAL (2w- and 8w-CAL) rats were measured and the myocardial SGs, Dys, calpain, and calpastatin levels were determined by the Western blot method. Myocardial calpain-like protease activity was evaluated as caseinolysis activity. **Results:** Increases in left ventricular end-diastolic pressure (LVEDP) and right ventricular systolic pressure, and a decrease in $\pm dP/dt$ were observed at the 2nd week, whereas cardiac output index (COI) was preserved. In contrast, the 8w-CAL rats showed a further increment in LVEDP with low COI. α-SG of the viable left ventricle (LV), and septum (Sep) of the 8w-CAL rat decreased (60–70% of the control). The α- and β-SGs of the right ventricle (RV) of the 2w- and 8w-CAL rats were reduced, while γ- and δ-SGs in the three regions did not change significantly. Dys in the viable LV and RV of the 8w-CAL rat decreased (75% of the control). The amount of *m*-calpain in the three regions of the 2w- and 8w-CAL rats increased (140–200% of the control), whereas the endogenous calpain inhibitor, calpastatin, did not change significantly. The in vitro degradation studies using purified *m*-calpain or cytosolic fractions of the 8w-CAL rat heart suggested a reduction in SGs and Dys by calpain. **Conclusion:** The results suggest that a decrease in SGs and Dys may play an important role in the pathophysiology of CHF following AMI.

Keywords: Calpain; Dystrophin; Heart failure; Hemodynamics; Sarcoglycan

1. Introduction

Dystrophin-related protein (DRP) complex consists of dystrophin, sarcoglycans, and dystroglycans and stabilizes sarcolemmal integrity [1]. Inherent mutation of dystrophin gene causes Duchenne- or Becker-type muscular dystrophy and dilated cardiomyopathy (DCM) [2]. Limb-girdle muscular dystrophy (LGMD) is caused by mutation of sarcoglycan (SG) subunits or by the deficiency of SGs [3]. Thus, some phenotypes of LGMD may induce the sarcoglycanopathy [3]. Recent studies have shown that cardiomyopathy in Bio14.6 [4] and TO-2 strain hamsters, which mimic dilated cardiomyopathy of humans [5], is caused by the gene deletion of δ-SG [4,6]. These two strains share a common gene mutation with distinct clinical features [7]. Kawada et al. reported that δ-SG gene transfection with recombinant adeno-associated virus improves cardiac function and survival of TO-2 hamster [8,9]. These findings suggest that changes in DRP complex may play an important role in the maintenance of muscle contractility.

Our previous studies revealed that the coronary ligation of rats at the proximal artery resulted in chronic heart failure with low cardiac output [10–12]. However, no

*Corresponding author. Tel.: +81-426-76-4583; fax: +81-426-76-5560.
E-mail address: takeos@ps.toyaku.ac.jp (S. Takeo).

Time for primary review 28 days.

0008-6363/03/$ – see front matter
doi:10.1016/S0008-6363(03)00385-7

information is available concerning changes in DRP complex in this heart failure. To verify the hypothesis that cardiac failure following acute myocardial infarction is associated with alteration in DRP complex, we examined alterations in DRP complex in the failing heart and possible involvement of endogenous calpain or calcium-activated neutral protease [13] in the process of DRP disruption.

2. Methods

2.1. Animals

Male Wistar rats (SLC, Hamamatsu, Japan), weighing 210–240 g, were used in the present study. The animals were conditioned according to *The Guide for the Care and Use of Laboratory Animals* as promulgated by the National Research Council. The protocol of this study was approved by The Committee of Animal Use and Welfare of Tokyo University of Pharmacy and Life Science.

2.2. Operation

Myocardial infarction was produced in 49 rats by ligation of the left ventricular coronary artery (CAL rats) according to the method described previously [10]. Rats that revealed an abnormal Q wave (more than 0.3 mV) 1 day after the operation were used for the following experiment [11]. Among the coronary artery-ligated rats, 33 rats survived by the 1st week after surgery (approx. 65% of the operated animals). Three rats died between the 2nd and 8th week after surgery. Thirty sham-operated rats without coronary artery ligation (Sham rats) were treated in a similar manner.

2.3. Measurement of hemodymanic parameters

Measurements of in vivo hemodynamic parameters were performed by a method described previously [10]. Briefly, prior to the operation, and 2 and 8 weeks after the operation, the rats were anesthetized with a gas mixture of nitrous oxide/oxygen (3:1) and 0.5–2.5% enflurane. A microtip pressure transducer (SPC 320, Miller Instrument, Houston, TX) was introduced into the left ventricle through the right carotid artery to measure left ventricular systolic and end-diastolic pressures (LVSP and LVEDP, respectively). The arterial blood pressure was measured by means of a pressure transducer attached to a cannula placed into the right femoral artery. Heart rate (HR) measurements were triggered from changes in arterial blood pressure. After 30 min equilibration of the setting, the above parameters were recorded.

After determination of the left ventricular function, the microtip pressure transducer was introduced into the right ventricle through the right jugular vein to measure the right ventricular systolic pressure (RVSP) and the right ventricular end-diastolic pressure (RVEDP). The Po_2, Pco_2, and pH of the blood samples of the animals under the present experimental conditions ranged from 95 to 104 mmHg, from 37 to 42 mmHg, and from 7.41 to 7.45 ($n=5$), respectively.

In another set of experiments, we determined the aortic flow by the method described previously [10]. The rats were inhaled with a gas mixture of nitrous oxide/oxygen and enflurane as described above, intubated, and artificially respirated with air. After dissection of the right thorax, an electro-magnetic flow meter with a diameter of 2.0–2.5 mm (MFV-3100, Nihon Kohden, Tokyo) was placed around the thoracic aorta, and then the aortic blood flow was measured. The systemic blood pressure was monitored through a cannula inserted into the femoral artery, and the heart rate was measured through the pulse of the systemic blood pressure. Cardiac output index was calculated by dividing aortic flow by body weight. The Po_2, Pco_2, and pH of the blood samples of the animals under the present experimental conditions ranged from 93 to 99 mmHg, 35 to 39 mmHg, and 7.38 to 7.42 ($n=5$), respectively.

2.4. Infarct size

After measurement of aortic flow, the left ventricle of rats with CAL or sham-operated rats was isolated and sectioned into seven slices with 1-mm thickness ($n=5$) from the base of the heart to the apex in a plane parallel to the atrioventricular groove. The slices were stained at 37 °C for 10 min with 1% triphenyltetrazolium chloride (TTC) in saline. After staining, TTC-unstained areas were determined according to a planimetric method [10].

2.5. Western blotting

Myocardial DRP complex proteins were determined by a modified method described previously [12]. Briefly, after determination of hemodynamic parameters for the left/right ventricular function, hearts were quickly isolated and then residual blood in the tissue was washed out with phosphate-buffered saline. The heart was divided into the left ventricular free wall without infarct area (viable LV), septum (Sep), and right ventricular free wall (RV). The tissues were homogenized in buffer containing 320 mM sucrose, 100 μM disodium EDTA, 100 μM phenylmethanesulfonyl fluoride (PMSF), and 10 mM Tris–HCl (pH 7.40). The homogenates were sampled for Western blot analysis. The samples were boiled in the Laemmli buffer containing 250 mM Tris–HCl, 4% SDS, 10% glycerol, 0.006% bromophenol blue, and 2% β-mercaptoethanol (pH 6.8), and fractionated by SDS electrophoresis on a 10% polyacrylamide gel (SDS–PAGE, 10×10 cm) for SGs, calpain, and calpastatin and on a 4% SDS–PAGE for dystrophin, respectively, according to the method of Laemmli [14].

The proteins separated on the gel were transferred on the PVDF membrane and then detected with their respective antibodies [11]. The following antibodies were used: anti-α-SG (1:1500 dilution; NCL-a-SARC, Novocastra Lab, Newcastle upon Tyne, UK), anti-β-SG (1:2000 dilution; NCL-b-SARC, Novocastra Lab), anti-γ-SG (1:3000 dilution; NCL-g-SARC, Novocastra Lab), anti-δ-SG (1:4000 dilution) [8], anti-dystrophin (1:3000 dilution; NCL-DYS1, Novocastra Lab), anti-*m*-calpain (1:3000 dilution; SA-255, Biomol, Plymouth Meeting, PA), and anti-calpastatine (1:1000 dilution; MAB3084, Chemicon, Temecula, CA). Thereafter, the proteins on the membrane were visualized by use of an ECL™ (Amersham Pharmacia Biotech, Buckinghamshire, UK) and their bands, developed on the X-ray films, were semi-quantified by a Densitograph® (Atto, Tokyo).

2.6. Preparation of sarcolemmal fraction

Crude sarcolemmal fraction was prepared from the left ventricular muscle of control rats including the septum as described previously [11]. The heart was homogenized with five volumes of cold buffer (300 μM PMSF, 320 mM sucrose, 1 mM EGTA, 20 mM Tris–HCl; pH 7.40). The homogenate was centrifuged at 1000×*g* at 4 °C for 10 min. The supernatant fluid was centrifuged at 8000×*g* for 20 min at 4 °C, and then the resultant supernatant fluid was recentrifuged at 100,000×*g* at 4 °C for 20 min. The resultant pellet was resuspended in the buffer without PMSF. The protein concentration was determined by the method of Lowry et al. [15].

2.7. Incubation of sarcolemma with m-calpain

To examine proteolysis of SGs and dystrophin by *m*-calpain, the sarcolemma-enriched fraction was incubated in the presence and absence of 10 mM $CaCl_2$ at 30 °C for 10–60 min in the reaction buffer of the following composition; 100 mM KCl, 10 mM β-mercaptoethanol, 5 U calpain II [rat recombinant calpain II (Calbiochem, San Diego, CA)], 5 mM $CaCl_2$, 20 mM Tris–HCl, pH 7.40. The reaction was terminated by the addition of 100 μM leupeptin, an exogenous cystein-protease inhibitor [13]. SG and dystrophin contents in the buffer were determined by Western blotting as described above.

2.8. Proteolytic activity ex vivo in cytosolic fraction

Caseinolytic activity of the cytosolic fraction, where calpain is present, isolated from the viable LV, Sep, and RV of the failing heart was estimated ex vivo using the degradation rate of casein. The tissue was homogenized with five volumes of 100 mM imidazole buffer (pH 7.50). The homogenate was centrifuged at 1000×*g* for 10 min at 4 °C. The supernatant was centrifuged at 8000×*g* for 20 min at 4 °C, and then the resultant supernatant fluid was recentrifuged at 100,000×*g* for 20 min at 4 °C. The supernatant fluid was used as a cytosolic fraction. Protein in each cytosolic fraction was incubated in the buffer of the following composition; 0.4% (w/v) casein, 5 mM cysteine, 5 mM $CaCl_2$, 100 mM imidazole/HCl (pH 7.5). After a 30 min-incubation, the reaction was terminated by the addition of ice-cold 5% (w/v) trichloroacetic acid and then the reaction mixture was centrifuged at 10,000×*g* for 15 min at 4 °C. The absorbance of the resultant supernatant at 280 nm, which represents small peptide fragments with aromatic amino acids produced by calpain proteolysis, was measured by a spectrophotometer (U-Best 30, JASCO, Hachioji, Japan). To determine the specificity for caseinolytic activity of calpain, leupeptin was added by 100 μM for the control activity.

Furthermore, the cytosolic fraction isolated from the viable LV, Sep, or RV of the 8w-CAL rat was incubated with the sarcolemmal fraction isolated from normal rats, and then sarcoglycan and dystrophin proteins after the incubation were determined by the method described above.

2.9. Experimental groups

In the present study, 30 CAL rats were used. Hemodynamic parameters of the 2w- and 8w-CAL rats ($n=6$ each) were measured and followed by determination of DRP complex proteins, calpain, and calpastatin. In another set of experiments, measurement of cardiac output index and subsequent determination of infarct size were carried out in the 2w- and 8w-CAL rats ($n=5$ each). The effect of leupeptin on caseinolytic activity of the cytosolic fraction of the 8w-CAL rats was determined ($n=4$). Proteolysis of DRP complex in the presence of the cytosolic fraction of the 8w-CAL rat was also determined ($n=4$).

2.10. Statistics

The results were expressed as the means±S.E.M. Statistical significance was estimated by analysis of variance (ANOVA) followed by Fisher's multiple comparison. Differences with a probability of less than 5% were considered to be statistically significant ($P<0.05$).

3. Results

3.1. Body, heart, and lung weight

Body weight of the CAL rat slightly but significantly decreased compared with that of the Sham rat (Table 1). Heart weight, heart weight-to-body weight ratio, RV weight, RV weight-to-body weight ratio of the CAL rat were larger than those of the Sham rat. Lung weight and lung weight-to-body weight ratio were also larger than those of the Sham rat.

Table 1
Cardiac and lung weight parameters of the Sham and CAL rats at the 2nd and 8th weeks after the operation

	Sham		CAL	
	2nd	8th	2nd	8th
BW (g)	256±3	320±6	230±5*	293±4*
LV (mg)	510±10	603±10	510±20	608±18
LV/BW (mg/g)	2.07±0.08	1.91±0.04	2.13±0.07	2.04±0.05
RV (mg)	140±10	160±3	231±10*	291±11*
RV/BW (mg/g)	0.53±0.02	0.49±0.01	0.97±0.06*	0.97±0.04*
Heart/BW (mg/g)	2.56±0.05	2.40±0.04	3.12±0.07*	3.11±0.07*
Lung (g)	0.99±0.03	1.02±0.01	2.40±0.10*	2.93±0.15*
Lung/BW (mg/g)	3.59±0.12	3.20±0.06	9.97±0.61*	9.96±0.43*
Infarct size (% LV)	N.D.	N.D.	41.8±1.7*	42.3±0.7*

Values except for infarct size represent the means±S.E.M. of six experiments. The value for infarct size represents the means±S.E.M. of five experiments. *Significantly different from the corresponding Sham group ($P<0.05$). Abbreviation: BW, body weight; LV, left ventricle; RV, right ventricle; N.D., not detectable.

3.2. Hemodynamics

The mean arterial pressure (MAP) and LVSP of the 2w- and 8w-CAL rats was decreased, whereas HR did not change significantly (Table 2). In contrast, the LVEDP of the CAL rat was increased at the 2nd week and elevated further at the 8th week. The RVSPs of the CAL rats were increased at the 2nd and 8th weeks compared with those of the Sham rat, whereas the RVEDPs of these CAL rats did not differ from the corresponding Sham rat. There were no significant differences in these parameters between the 2w- and 8w-Sham rats.

In another set of experiments, cardiac output index was determined. Cardiac output index of the CAL rat decreased at the 8th week, whereas it did not alter at the 2nd week (Table 2). There were no changes in the cardiac output index of Sham rats throughout the experiment. The infarct area of the CAL rat occupied approximately 40% of the left ventricle (Table 1), but no infarction in the myocardium of Sham rats was seen.

3.3. Expression of SGs in myocardium

After the in vivo measurement of hemodynamics, the contents of myocardial SG and dystrophin proteins in the viable LV, Sep, and RV were quantified by the Western blot method (Fig. 1). α-SG content in the RV of the 2w-CAL rat decreased, whereas that of the viable LV or Sep did not alter. Myocardial α-SG content in all three portions of the 8w-CAL rat decreased to approximately 60, 70, and 55% of the control value, respectively. β-SG content in the RV of the 2w- and 8w-CAL rats decreased, whereas those in the viable LV and Sep of either CAL rat did not change significantly. γ- and δ-SGs in the three portions of the CAL rat remained constant throughout the experiment. These four SGs in the heart of the Sham rat were similar to those of the control.

There were no changes in dystrophin content in the three portions of the 2w-CAL rat. Dystrophin contents in the viable LV and RV of the 8w-CAL rat decreased to approximately 85% and 75% of the control. Dystrophin

Table 2
Hemodynamic parameters of the Sham and CAL rats at the 2nd and 8th weeks after the operation

	Sham		CAL	
	2nd	8th	2nd	8th
MAP (mmHg)	109±2	120±2	104±3*	112±3*
Heart rate (beats/min)	401±1	400±1	398±1	399±1
LVSP (mmHg)	140±2	158±3	133±3	144±3*
LVEDP (mmHg)	1.8±0.6	0.8±0.3	21.8±1.6*	31.5±0.9*
LV+dP/dt (mmHg/s)	11,092±569	12,578±374	7729±441*	8559±441*
LV−dP/dt (mmHg/s)	9992±357	11,737±416	7729±215*	5219±263*
COI (ml/min per kg)	201±14	195±16	186±11	137±10*
RVSP (mmHg)	28.4±2.1	22.1±1.3	67.7±6.5*	65.9±5.6*
RVEDP (mmHg)	0.4±0.1	0.6±0.2	0.7±0.2	0.8±0.3

Values for hemodynamic parameters except for COI represent the means±S.E.M. of six experiments. The value for COI represents the means±S.E.M. of five experiments. *Significantly different from the corresponding Sham group ($P<0.05$). Abbreviations: MAP, mean arterial pressure; LVSP, left ventricular systolic pressure; LVEDP, left ventricular end-diastolic pressure; COI, cardiac output index; RVSP, right ventricular systolic pressure; RVEDP, right ventricular end-diastolic pressure.

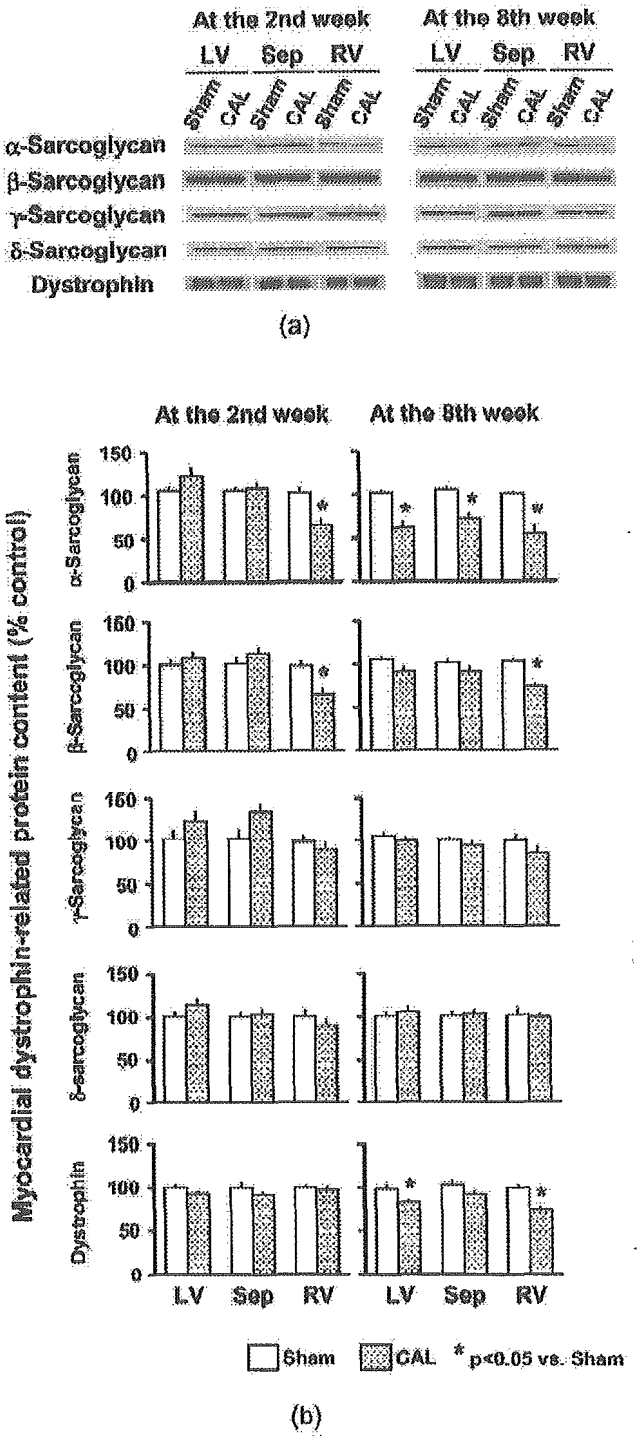

Fig. 1. Representatives of Western blot analysis (A) and semi-quantified data (B) for α-, β-, γ-, and δ-sarcoglycan, and dystrophin proteins in the viable left ventricular free wall (LV), intermediate septum (Sep), and right ventricular free wall (RV) of the Sham (open columns) and CAL rats (hatched columns) at the 2nd (left panels) and 8th weeks (right panels) after the operation. Each value represents the mean±S.E.M. of six experiments. *Significantly different from the corresponding Sham group ($P<0.05$).

content in the Sep of the 8w-CAL rat tended to be decreased. Myocardial dystrophin content in the three portions of the Sham rat was similar to that of the control throughout the experiment.

3.4. Amount of myocardial calpain and calpastatin

Changes in myocardial calpain and calpastatin of the operated rats are shown in Fig. 2. Calpain content of the viable LV, Sep, and RV of the 2w-CAL rat increased to approximately 165, 140, or 205% of the control, respectively. Calpain content of these three regions in the 8w-CAL rat also increased to a level similar to those of the 2w-CAL rat. In contrast, calpastatin content of the heart remained unchanged in the 2w- and the 8w-CAL rats. There were no significant changes in myocardial calpain and calpastatin contents in the Sham rat.

3.5. Incubation of sarcolemma with calpain

Changes in SGs and dystrophin proteins of the sarcolemmal fraction in the presence of *m*-calpain are shown in Fig. 3. When the sarcolemmal fraction from normal hearts was incubated with rat recombinant *m*-calpain, α-SG decreased to 50, 20, and 15% of the control (in the absence of calpain) at 5, 10, and 15 min after starting the

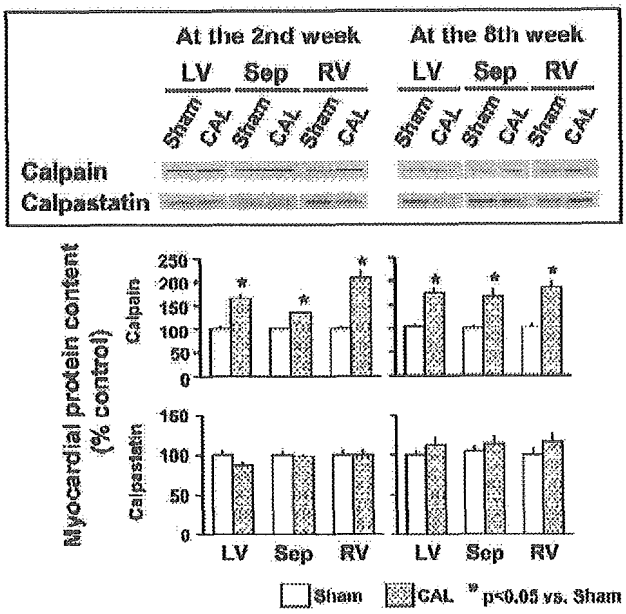

Fig. 2. Representatives of Western blot analysis (upper panels) and semi-quantified data (lower panels) for *m*-calpain and calpastatin proteins in the viable left ventricular free wall (LV), intermediate septum (Sep), and right ventricular free wall (RV) of the Sham (open columns) and CAL rats (hatched columns) at the 2nd (left panel) and 8th weeks (right panel) after the operation. Each value represents the mean±S.E.M. of six experiments. *Significantly different from the corresponding Sham group ($P<0.05$).

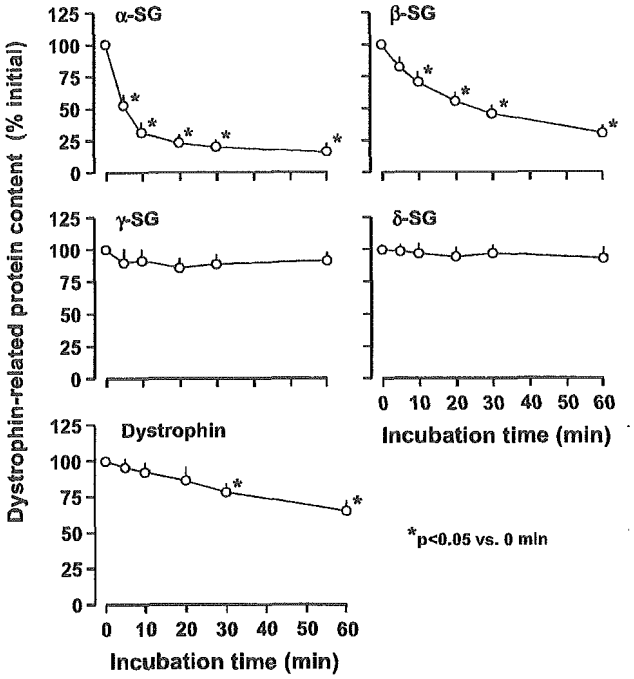

Fig. 3. Time course of changes in α- (α-SG; upper left), β- (β-SG; upper right), γ- (γ-SG; middle left), and δ-sarcoglycan proteins (δ-SG; lower right), and dystrophin (lower left) of the isolated sarcolemmal fraction in the presence of rat recombinant *m*-calpain. Each value represents the mean±S.E.M. of four experiments. *Significantly different from pre-incubation value (0 min; $P<0.05$).

incubation, respectively. Although β-SG also decreased in the presence of calpain, the protein decreased more gradually than α-SG. In contrast, γ- and δ-SGs did not decrease within 30 min incubation in the presence of calpain. Dystrophin decreased 20 min after the onset of incubation, whereas this protein did not significantly decrease until 15 min after the incubation with calpain.

3.6. Calpain-like proteolytic activity

Differences in proteolytic activity in the cytosolic fraction between the Sham and CAL rat hearts were examined. The left panel in Fig. 4 shows changes in absorbance at 280 nm during incubation of the cytosolic fraction prepared from the viable LV of the 8w-CAL rat and the LV of the 8w-Sham rat. Incubation of casein with the cytosolic fraction prepared from the LV of the 8w-Sham rat resulted in a gradual increase in the absorbance at 280 nm in a time-dependent manner. When casein was incubated with Sep or RV of the 8w-Sham rat, the degree of increase in the absorbance was similar to that of LV (data not shown).

The increases in the absorbance at 280 nm during incubation of casein with the cytosolic fraction of the viable LV, Sep, or RV of the 8w-CAL rat were all greater than that of the 8w-Sham rat (the left panel in Fig. 4). The degree of caseinolytic activity in the cytosolic fraction of

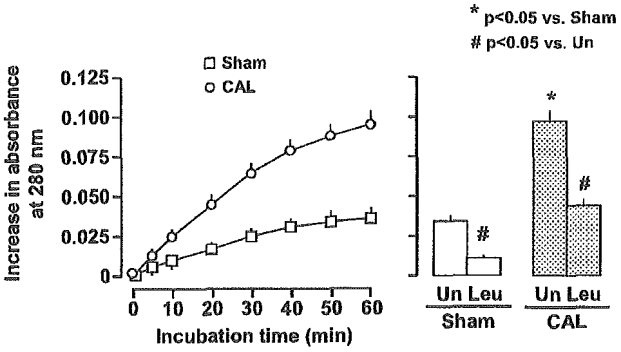

Fig. 4. Changes in casein proteolysis (caseinolysis) in the myocardial cytosolic fraction prepared from the Sham (square and open columns) or the 8w-CAL rat (circle and hatched columns) (left panel) and the effect of leupeptin (Leu) on the caseinolysis of the cytosolic fraction (right panel). Each value represents the mean±S.E.M. of four experiments. *Significantly different from the Sham rat (Sham; $P<0.05$). #Significantly different from leupeptin-untreated group (Un; $P<0.05$).

the Sep or RV of the 8w-CAL rat was similar to that of the viable LV (data not shown).

The right panel in Fig. 4 shows the effect of leupeptin, an exogenous calpain inhibitor, on the casein proteolysis in the cytosolic fraction prepared from the 8w-CAL rat heart. Increased caseinolytic activity of the 8w-CAL rat was attenuated by the presence of 100 μM leupeptin (to approx. 45% of the leupeptin-untreated value).

3.7. Incubation of the sarcolemma isolated from normal rat heart with cytosolic fraction from 8w-CAL rat heart

Fig. 5 shows myocardial sarcoglycan and dystrophin proteins released from the sarcolemmal fraction of normal rats upon incubation with the cytosolic fraction of the viable LV of the 8w-CAL rat. After 60-min incubation, α- and β-SGs, and dystrophin proteins reduced to approximately 40, 60, and 80% of the pre-incubation levels,

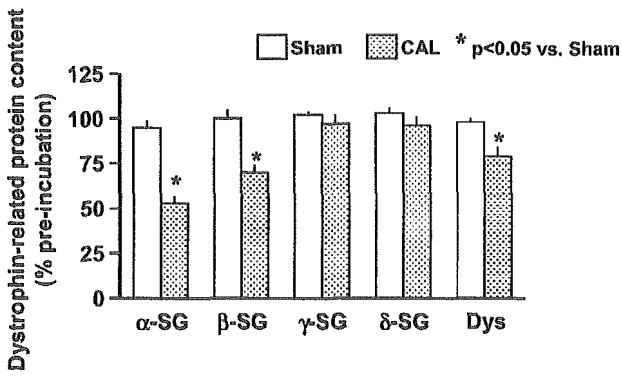

Fig. 5. Sarcoglycan and dystrophin proteins released from the isolated sarcolemmal fraction upon 60-min incubation with the cytosolic fraction of the viable left ventricle of the 8w-CAL (open columns) and 8w-Sham rats (dotted columns). Each value represents the mean±S.E.M. of four experiments. *Significantly different from pre-incubation value ($P<0.05$).

respectively. In contrast, γ- and δ-SGs after the incubation did not change. The sarcoglycans and dystrophin upon incubation with the cytosolic fraction from the 8w-Sham rat did not release. The degree of proteolytic activity in the cytosolic fraction of the Sep or RV of the 8w-CAL rat was similar to that of the viable LV (data not shown).

4. Discussion

Genetic defects of SGs and/or dystrophin may result in the development of cardiomyopathy and/or muscular dystrophies [2,3,6,16]. The roles of the changes in DRP complex of the heart without genetic mutation, however, have not been clarified. In the present study, we have shown for the first time that alterations in myocardial DRP complex are detected in failing hearts following acute myocardial infarction of the rat that has no genetic mutation of DRP complex.

We observed an increase in LVEDP and decreases in LVSP and $\pm dP/dt$ of the CAL rat at the 2nd week without a decrease in COI, suggesting that cardiac function of the 2w-CAL rat was compensated. In contrast, we found the further rise in LVEDP and a decline in COI of the CAL rat at the 8th week, suggesting signs for chronic heart failure (CHF) with low cardiac output as were the cases in previous studies [10–12]. We also found a marked increase in RVSP of both 2w- and 8w-CAL rats without any change in RVEDP. In addition, the lung weight of the CAL rats for both periods increased. These changes may be more or less linked to hypertrophy of the right ventricular free wall of the CAL rat.

We found diverse changes in SG complexes in the failing heart, i.e. α-SG content of the viable LV and Sep of the 8w-CAL rat decreased, whereas α- and β-SG contents decreased only in the RV of the 2w- and 8w-CAL rats. Dystrophin content was decreased in the LV and RV of the 8w-CAL rat, but not of the 2w-CAL rat. In contrast, γ- and δ-SGs in the three portions remained constant throughout the experiment. The findings showed that α-SG content was decreased most prominently among the SG proteins and that alterations in α-SG and dystrophin were associated with the genesis of chronic heart failure with low cardiac output. These results suggest that decreases in α-SG and dystrophin may play an important role in the pathophysiology of cardiac failure after CAL in rats. This is partially comparable to the previous findings that LGMD 2D, a muscular dystrophy, which reduces tolerance in exercise capacity [17], is caused by mutations in the α-SG gene [18].

β-SG in the RV of the 2w- and 8w-CAL rats decreased, whereas β-SG in the viable LV and Sep did not change significantly. Zimmer et al. suggest that in this rat model, the left ventricular muscle is capable of adapting to volume overload and the right ventricular muscle, to pressure overload [19]. In accordance with this, we observed that functional failure in either ventricle of the CAL rat was associated with the alterations in β-SG. Thus, the changes in β-SG may contribute to the genesis of contractile dysfunction of the CHF animals. This may account for an increase in RVSP, an indication of right ventricular dysfunction of the 8w-CAL animals.

Questions arise regarding the mechanism underlying the decreases in SGs and dystrophin after CAL. In this context, we focused on proteolysis of the components in the DRP complex. We found an increase in *m*-calpain protein in the failing heart, which is one of the Ca^{2+}-dependent neutral cysteine proteases present in all mammalian cells. Sandmann et al. reported that transcription and translation of calpain in the viable left ventricular muscle were increased after myocardial infarction [20]. We found an increase in *m*-calpain of the viable LV, Sep, and RV in the failing heart at both the 2nd and 8th weeks after myocardial infarction. Calpain content in the RV of the 2w-CAL rat was greater than those in the viable LV and Sep, and β-SG in the RV, but not in the viable LV and Sep of the 2w-CAL rat was decreased. In contrast, calpastatin, an endogenous inhibitor of calpain, in the failing heart was constant. Since calpastatin has been shown to fully inhibit proteolytic activity of all calpain isoforms at a 1:1 ratio of calpain to calpastatin [21], the predominant increase in calpain with no significant changes in calpstatin in the CAL animal may lead to relative enhancement of proteolytic activity for the intracellular proteins such as DRP complex.

Furthermore, we found higher caseinolytic activity in the myocardial cytosolic fraction of the rat with CHF. The study on the incubation with the sarcolemmal fraction from control animals showed a rapid decrease in α-SG, a gradual decrease in β-SG, and a more delayed decrease in dystrophin. In contrast, γ- and δ-SGs were unchanged in the presence of calpain. These patterns of changes in DRP complex in the incubation with *m*-calpain are comparable with those of DRP complex content in the failing heart. We found calpain-induced increase in the caseinolytic activity in the cytosolic fraction of the 8w-CAL rat heart, which was partially attenuated by a calpain inhibitor leupeptin. Furthermore, the cytosolic fraction of the 8w-CAL rat heart also showed enhanced degradation of DRP complex proteins. These results suggest that the increase in calpain levels relative to calpastatin in the failing heart may contribute to decreases in α- and β-SGs and dystrophin during the development of heart failure.

In the present study, we found a greater degree of the decrease in α-SG in the failing heart than that in β-SG and dystrophin. Yoshida et al. [22,23] showed that β-, γ-, and δ-SG were cross-linked by succinimidyl propionate, whereas α-SG was not linked to others. The three SGs except α-SG have the N-terminal in the intracellular space and a large extracellular domain including a cystein-rich cluster near the C-terminal regions [1]. In contrast, α-SG has the C-terminal amino acid residue in the intracellular

space and a cystein-rich cluster near the transmembrane domain [1]. Therefore, it is likely that the structure of α-SG in the sarcolemma may have high affinity to the intracellular proteases such as calpain.

γ- and δ-SGs contents in the failing heart were similar to those of the heart in the Sham rats. Incubation with purified calpain did not alter γ- and δ-SGs in the isolated sarcolemma. Nigro et al. showed that amino acid sequences of γ-SG revealed approximately 55% amino acid identity and approximately 70% similarity to that of δ-SG [24]. Thus, these SGs may have structures and/or location in the sarcolemma with high tolerance to calpain-induced proteolysis.

In summary, we found that the DRP complex in the failing heart following AMI was altered in rats without genetic defects. The acquired reduction was detected in the viable LV, Sep, and RV. The non-proportional decreases in α- and β-SGs and dystrophin may result in a reduction in the amount of functional DRP complex in the sarcolemma, suggesting that a decrease in DRP complex may play an important role in the genesis of contractile dysfunction in heart failure. The advanced heart failure following AMI may be developed by multiple decreases in DRP proteins, but not by a decrease in single protein. The present ex vivo and in vitro findings also suggest that calpain may contribute to a decrease in DRP complex.

Acknowledgements

This work was partly supported by the Grants of the Promotion and Mutual Aid Corporation for Private Schools of Japan, and of Ministry of Education, Culture, Sports, Science and Technology.

References

[1] Ozawa E, Noguchi S, Mizuno Y, Hagiwara Y, Yoshida M. From dystrophinopathy to sarcoglycanopathy: evolution of a concept of muscular dystrophy. Muscle Nerve 1998;21:421–438.
[2] Kunkel LM. Analysis of deletions in DNA from patients with Becker and Duchenne muscular dystrophy. Nature 1986;11:73–77.
[3] Melacini P, Fanin M, Duggan DJ, Freda MP, Berardinelli A, Danieli GA, Barchitta A, Hoffman EP, Dalla Volta S, Angelini C. Heart involvement in muscular dystrophies due to sarcoglycan gene mutations. Muscle Nerve 1999;22:473–479.
[4] Nigro V, Okazaki Y, Belsito A, Piluso G, Matsuda Y, Politano L, Nigro G, Ventura C, Abbondanza C, Molinari AM, Acampora D, Nishimura M, Hayashizaki Y, Puca GA. Identification of the Syian hamster cardiomyopathy gene. Hum Mol Genet 1997;6:601–607.
[5] Tsubata S, Bowles KR, Vatta M, Zintz C, Tius J, Muhonen L, Bowles NE, Towbin JA. Mutations in human δ-sarcoglycan gene in familial and sporadic dilated cardiomyopathy. J Clin Invest 2000;106:655–662.
[6] Sakamoto A, Ono K, Abe M, Jasmin G, Eki T, Murakami Y, Masaki T, Toyo-oka T, Hanaoka F. Both hypertrophic and dilated cardiomyopathies are caused by mutation of the same gene, delta-sarcoglycan, in hamster: an animal model of disrupted dystrophin-associated glycoprotein complex. Proc Natl Acad Sci USA 1997;94:13873–13878.
[7] Whitmer JT, Kumar P, Solaro RJ. Calcium transport properties of cardiac sarcoplasmic reticulum from cardiomyopathic Syrian hamsters (BIO 53.58 and 14.6): evidence for a quantitative defect in dilated myopathic hearts not evident in hypertrophic hearts. Circ Res 1988;62:81–85.
[8] Kawada T, Sakamoto A, Nakazawa M, Urabe M, Masuda F, Hemmi C, Wang Y, Shin WS, Nakatsuru Y, Sato H, Ozawa K, Toyo-oka T. Morphological and physiological restorations of hereditary form of dilated cardiomyopathy by somatic gene therapy. Biochem Biophys Res Commun 2001;284:431–435.
[9] Kawada T, Nakazawa M, Nakauchi S, Yamazaki K, Shimamoto R, Urabe M, Nakata J, Hemmi C, Masui F, Nakajima T, Suzuki J, Monahan J, Sato H, Masaki T, Ozawa K, Toyo-oka T. Rescue of hereditary form of dilated cardiomyopathy by rAAV-mediated somatic gene therapy: amelioration of morphological findings, sarcolemmal permeability, cardiac performances, and the prognosis of TO-2 hamsters. Proc Natl Acad Sci USA 2002;99:901–906.
[10] Sanbe A, Tanonaka K, Hanaoka Y, Katoh T, Takeo S. Regional energy metabolism of failing heart following myocardial infarction. J Mol Cell Cardiol 1993;25:995–1013.
[11] Yoshida H, Tanonaka K, Miyamoto Y, Abe T, Takahashi M, Anand-Srivastava MB, Takeo S. Characterization of cardiac myocyte and tissue b-adrenergic signal transduction in rats with heart failure. Cardiovasc Res 2001;50:34–45.
[12] Tanonaka K, Furuhama K, Yoshida H, Kakuta K, Miyamoto Y, Takeo S. Protective effect of heat shock protein 72 on the contractile function of the perfused failing heart. Am J Physiol 2001;281:H215–H222.
[13] Toyo-oka T, Shimizu T, Masaki T. Inhibition of proteolytic activity of calcium activated neutral protease by leupeptin and antipain. Biochem Biophys Res Commun 1978;82:484–491.
[14] Laemmli UK. Cleavage of structural proteins during the assembly of the head of bacteriopharge T4. Nature 1970;277:680–685.
[15] Lowry OH, Rosebrough NJ, Farr AL, Randall RJ. Protein measurement with the folin phenol reagent. J Biol Chem 1951;261:6300–6306.
[16] Megeney LA, Kablar B, Perry RLS, Ying C, May L, Rudnicki MA. Severe cardiomyopathy in mice lacking dystrophin and MyoD. Proc Natl Acad Sci USA 1999;96:220–225.
[17] Mongini T, Doriguzzi C, Bosone I, Chiado-Piat L, Hoffman EP, Palmucci L. α-Sarcoglycan deficiency featuring exercise intolerance and myoglobinuria. Neuropediatrics 2002;33:109–111.
[18] Roberds SL, Leturcq F, Allamand V, Piccolo F, Jeanpierre M, Anderson RD, Lim LE, Lee JC, Tome FMS, Romero NB, Fardeau M, Beckmann JS, Kaplan J-C, Campbell KP. Missense mutations in the adhelin gene linked to autosomal recessive muscular dystrophy. Cell 1994;78:625–633.
[19] Zimmer HG, Gerdes AM, Lortet S, Mall G. Changes in heart function and cardiac cell size in rats with chronic myocardial infarction. J Mol Cell Cardiol 1990;22:1231–1243.
[20] Sandmann S, Yu M, Unger T. Transcriptional and translational regulation of calpain in the rat heart after myocardial infarction—effects of AT_1 and AT_2 receptor antagonists and ACE inhibitor. Br J Pharmacol 2001;132:767–777.
[21] Suzuki K, Imajoh S, Emori Y, Kawasaki H, Minami Y, Ohno S. Calcium activated neutral protease and its endogenous inhibitor: activation at the cell membrane and biological function. FEBS Lett 1987;220:271–277.
[22] Yoshida M, Suzuki A, Yamamoto H, Noguchi S, Mizuno Y, Ozawa E. Dissociation of the complex of dystrophin and its associated proteins into several unique groups by *n*-octyl β-D-glucoside. Eur J Biochem 1994;222:1055–1061.

[23] Yoshida M, Noguchi S, Wakabayashi E, Piluso G, Belstio A, Nigro V, Ozawa E. Biochemical identification of δ-sarcoglycan. FEBS Lett 1997;403:143–148.
[24] Nigro V, Piluso G, Belsito A, Politano J, Puca AA, Papparella S, Rossi E, Viglietto G, Esposito MG, Abbondanza C, Medici N, Molinari AM, Nigro G, Puca GA. Identification of a novel sarcoglycan gene at 5q33 encoding a sarcolemmal 35 kDa glycoprotein. Hum Mol Genet 1996;5:1179–1186.

High Fidelity SNP Genotyping Using Sequence-Specific Primer Elongation and Fluorescence Correlation Spectroscopy

K. Hori[1,*], W.S. Shin[3], C. Hemmi[3], T. Toyo-oka[2,3] and T. Makino[1]

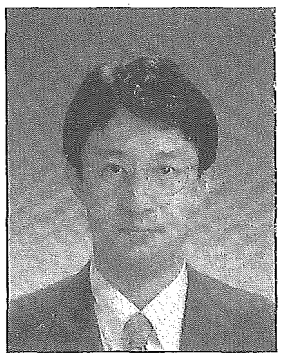

[1]*NovusGene Inc.*, [2]*Department of Pathophysiology and Internal Medicine, University of Tokyo*, [3]*Health Service Centre, University of Tokyo, Japan*

Abstract: Reliable, efficient and cost-effective modalities are urgently needed for mass screening of gene mutations. Previous reports have shown that SSCP or genechip methods require substantial time and monetary costs, thus limiting their appeal. Sequence Specific Primer Polymerase Chain Reaction (SSP-PCR) is a reliable and cost-effective method that utilizes the 3'-end discrimination properties of polymerase. However, the applicability of conventional SSP-PCR is limited due to the difficulties associated with determining optimal conditions and because mis-matched primers are amplified, resulting in signal noise during end-point assay. To overcome this problem, we eliminated the reverse primers from SSP-PCR, thus preventing amplification of mis-matched primers. We designated this method Sequence-Specific Primer Cycle Elongation (SSPCE). However, the detection of elongated sequence specific primers was difficult using conventional electrophoresis due to the small amounts of amplification product present. We therefore combined SSPCE and Fluorescence Correlation Spectroscopy, which is a novel technique used to determine the number and size of fluorophores at nano-molar concentrations, and designated the method SSPCE-FCS. We compared conventional SSP-PCR and SSPCE-FCS with regard to determining optimal conditions using two Mitochondrial SNPs (G $\rightarrow$ A at position 1598, G $\rightarrow$ A at position 12192). We were able to determine the optimal conditions for the SNP at position 1598 using either method. However, optimal conditions could only be determined for SSPCE-FCS with the 12192 mutation because non-specific amplification was observed at a wide range of annealing temperatures in SSP-PCR. We then applied this method to three other SNPs and the results were consistent with the results of sequencing data.

Key Words :Single Nucleotide Polymorphism (SNP), Mutation, Fluorescence Correlation Spectroscopy (FCS), Hypertrophic Cardiomyopathy.

INTRODUCTION

Single nucleotide polymorphisms (SNPs) are useful as DNA markers in population genetics, and for mapping candidate genes to detect disease susceptibility [1]. To utilize this potential, the development of low-cost and high-throughput technology has been required. This technology includes TaqMan, Molecular beacons, Scorpion primers, sequence specific primer PCR (SSP-PCR), pyrosequencing and oligonucleotide ligation assay. However, laborious separation steps are necessary for some of these methods while expensive and difficult primer design for precise genotyping is necessary for others.

Fluorescence correlation spectroscopy (FCS) is a novel technique for determining the size and number of fluorophores based on the autocorrelation function of fluorescence intensity signals caused by Brownian motion of fluorophores through the confocal volume defined by an excitation laser focused with confocal optics. The theory and concept were developed in the early 70's [2] and have been exploited in a variety of applications [3,4], including detection of PCR products [5,6] and hybridization of DNA [7]. The principles will be described elsewhere in this volume. For SNP genotyping, modified SSP-PCR has been used in conjunction with FCS [8,9]. In this method, small concentrations of two different fluorophore-labeled sequence-specific primers and the usual forward and reverse primers are used simultaneously. This is one of the most powerful methods for genotyping in one tube, although non-specific amplification, which is an intrinsic problem with SSP-PCR, still occurs.

SSP-PCR is based on differences in the primer extension efficiency of *Thermus aquaticus* (*Taq*) DNA polymerase with a primer having a matched or mismatched 3'-terminus. It was demonstrated that the extension efficiency is 10^{-3} to 10^{-4} for a transition mismatch and 10^{-5} to 10^{-6} for a transversion mismatch [10]. During PCR amplification, if a single mismatch occurs, the product becomes a template and is subsequently amplified as a non-specific product. However, the non-specific amplification rate is lower than that for a perfect match, and thus kinetic PCR has been used to detect the difference between these rates. Because the amplification profiles of kinetic PCR are different for each SNP genotype, profile data is required for each SNP. The time required for genotyping is the same as that needed for PCR itself. For high-throughput genotyping, end-point assay may first be required.

When there is no reverse primer in SSP-PCR, only the elongation of primers occurs. Under these conditions, if a mismatched primer is elongated, there is no further amplification. If the sequence-specific primers are labeled with fluorescence, those that are elongated and those that are not

*Address correspondence to this author at the Novus Gene Inc., 2-3 Kuboyama-cho, Hachioji-shi, Tokyo, 192-8512, Japan; Tel: +81-426-96-4330; Fax: +81-426-91-6035; E-mail: hori-k@novusgene.co.jp

1389-2010/03 $41.00+.00

elongated are easily discriminated by FCS. We designated this method "Sequence Specific Primer Cycle Elongation (SSPCE)". By combining SSPCE and FCS (SSPCE-FCS), the 3'-terminus discriminatory properties of *Taq* polymerase are fully exploited. In the present paper, we report the genotyping of four transversion SNPs and one transition SNP, and demonstrate that the results are consistent with sequence data.

SNP GENOTYPING METHODS

Numerous genotyping methods have been proposed and developed. As several reviews were presented previously [11-13], we describe some of representative methods here. These can be broadly categorized as either non-enzymatic or enzymatic. One of the non-enzymatic methods is hybridization. In this method, oligo probes are designed to hybridize with the desired sequence and the genotype is easily discriminated by adjusting the optimal hybridization conditions. Genechip (Affimetrix) is a hybridization method in which oligo probes are fixed on a solid support [14]. The advantage is that thousands of SNPs may be screened simultaneously. However, designing the oligo probes is difficult because the hybridization conditions must be the same for all SNPs being screened, and thus this technique is not suited for genotyping several SNPs in numerous samples. PNA (Peptide Nucleic Acids) [15] and LNA (Locked Nucleic Acids) probes [16], which have high affinities for complimentary DNA and thus allow shorter probes to be used, have also been used in this solid support method. Although these probes may improve the specificity of hybridization, they cost more than DNA probes.

In order to minimize the difficulties associated with designing oligo probes, DASH (Dynamic Allele-Specific hybridization) was proposed [17]. In this method, target DNA is captured on avidin-coated microtiter plates after PCR with biotinylated primers. On microtiter plates, oligo probes were hybridized with captured target DNA and intercalating fluorescence dyes. When elevating the annealing temperature, it is possible to monitor the changes in the fluorescent signal profile with increasing temperature, and use these profiles to detect matched and mismatched hybridization. Designing oligo probes is much easier for this method than for other methods because the conditions for observing each SNP are the same. However, capturing DNA on macriotiter plates is laborious and has a lower throughput than other solid support hybridization techniques.

Other hybridization techniques that are assisted by polymerases are Taqman or molecular beacon [18, 19]. In these methods, the allele-specific probes used are FRET (Fluorescent Resonance Energy Transfer) probes. FRET probes contain a fluorescent reporter at the 5'-terminus, and a FRET moiety at the 3'-terminus that quenches the fluorescent signals of the reporter. In the Taqman method, matched FRET allele-specific probes are cleaved by the 5'→3' exonuclease activity of *Taq* DNA polymerase, which releases the fluorescent reporter molecules, while mismatched probes are not cleaved during PCR. Thus, fluorescence signals are only observed for matched FRET probes. In reality, because the background signals increase in proportion to the number of thermal cycles as a result of accumulation of fluorescent reporters cleaved from mismatched probes, real-time monitoring is necessary. Molecular beacons are labeled in the same manner as Taqman FRET probes except that the sequences are complimentary at the 3'- and 5'-termini, thus generating stem-loop structures adjacent to the fluorescence reporter. This structure is advantageous when compared to the linear Taqman probe for energy transfer, and provides numerous reporter-quencher combinations. In real-time PCR using molecular beacons, when probes are matched the SNP site, fluorescent signals are increased because the reporters are free from quenchers as the stem-loop structures are linearized. These FRET probe-based PCR methods have lower throughput than the hybridization assays, but sensitivity and specificity may be increased by real-time monitoring of hybridization events. These hybridization techniques depend on the thermodynamics of the probe and target SNPs.

In contrast, enzymatic methods depend on the specificity of enzymes. OLA (Oligo Nucleotide Ligation Assay) relies on ligase to discriminate between matches and mismatches at the ligation site in two adjacently hybridized oligonucleotides. This method is used in LCR (Ligase Chain Reaction) or padlock probes [20, 21]. Invader assay uses structure-specific enzymes to cleave the complex formed by hybridization of overlapping oligonucleotide probes [22]. When probes are designed such that the polymorphic site is at the point of overlap, the correct overlapping structure is formed with the allele-specific probe but not with probes having any mismatch. Elevated temperatures and excess of the allele-specific probes enable the cleavage of multiple probes for each target sequence present in an isothermal reaction. The cleaved allele-specific probe can be detected directly or further amplified by a serial, isothermal Invader assay based on a FRET-labeled probe.

The ability of DNA polymerase to incorporate specific deoxyribonucleotides complementary to the target DNA sequence is utilized in single-base extension technology. MassEXTEND, developed by Sequenom, is one of the representative methods in this category [23]. In this method, the primer begins 2-3 nuculeotides upstream of the SNP site, and the primer extension reaction is conducted using a single ddNTP, which is specific to the SNP site, and the three remaining dNTPs. Addition of dNTPs allows the allele containing the common variant to be extended by past the SNP site. The extended primers are measured by TOF (Time of Flight) mass spectrometry. TOF mass spectrometry can readily distinguish between products differing in length by only a few nucleotides.

We have also utilized primer extension technology and combined it with fluorescent polarization [24]. In this method, a fluorescent-labeled ddNTP specific for the SNP base is incorporated into the primer, which binds immediately upstream from the SNP site, and the difference in fluorescent polarization between incorporated and unincorporated ddNTPs is detected.

Another variation of primer extension technology is known as Pyrosequencing [25]. In Pyorosequencing, primer extension is monitored by enzyme-mediated luminometeric detection of pyrophosphate, which is released upon incorporation of dNTP. The genotype of an SNP is deduced by sequential addition and degradation of nucleotides using

apyrase in a dedicated instrument that operates in a 96-well format or a 384-well microtiter plate format.

The ability of DNA polymerase to discriminate between primers having matched and unmatched 3'-termini at the target SNP site is utilized in SSP-PCR (Sequence Specific Primer PCR), which is also known as ARMS (Amplification refractory Mutation System) or Allele Specific PCR [26, 27]. In this method, PCR primers with the 3'-terminus complimentary to either of the nucleotides of an SNP are used in combination with common reverse primers selectively amplify SNP alleles. Originally this amplified product was detected by electrophoresis, but several variations have been developed to specifically detect amplified products. Scorpion primers have been used as SSP-PCR primers for homogeneous assay [28]. Scorpion primers are designed to link probe sequences to the 5'-terminus of the SSP-primer. The probe segment is designed to act as a FRET probe, in a similar way as in molecular beacon, and the sequence contains the complementary sequence to target DNA, which then hybridizes with the extended scorpion primer. In this method, fluorescence signals increase only when amplification occurs. Universal FRET primers have also been developed [29]. SSP-primers contain a universal 5'-tail sequence that becomes part of the PCR product on amplification. When SSP-PCR is conducted with a universal pair of secondary hairpin structured FRET primers, SSP-primers, and reverse primers, FRET primers are incorporated into amplification products and the fluorescence signal increases. The advantage of these methods is one-tube genotyping. However, scorpion primers are expensive as they require labeling at both primer ends. In the method using universal FRET primers, it is difficult to design appropriate primers because of the intrinsic assay complexity.

Fluorescence correlation spectroscopy (FCS) has been used in a one-tube genotyping assay called GALIOS (Gene Amplification and Labeling In One System) [9]. In this method, one pair of gene-specific amplification primers and two allele-specific fluorescent labeled primers are used in a semi-nested way. After PCR, the quantities of allele-specific fluorescent PCR products are determined by FCS. In conventional SSP-PCR, SSP-primers have two roles; one is the detection of SNPs and the other is to act as the forward primer in PCR. In order to increase the specificity of PCR, reverse primers may be designed stringently because the sequence of forward SSP-primer is fixed to the region adjacent to the SNP site. In GALIOS, because forward primers are only amplified the SNP region, designing primers is easier than for other SSP-PCR methods. However, the disadvantage of these SSP-PCR is that the miss-extended primer is easily amplified, thus increasing background signals.

SNP GENOTYPING BY SEQUENCE SPECIFIC PRIMER CYCLE ELONGATION (SSPCE)

One of the problems intrinsic to SSP-PCR is that the reaction conditions and primer design for selective amplification should be empirically optimized for each SNP. This is largely the result of non-specific amplification of the sequence specific primers. To overcome this, we have eliminated the reverse primers from SSP-PCR, thus optimizing conditions and increasing the range of usable annealing temperatures when compared to conventional SSP-PCR (Fig. (**1**)).

We demonstrate here the genotyping of three mitochondrial SNPs (G → A at position 1598 [30], G → A at position 12192 [31] and G → A at position 15927

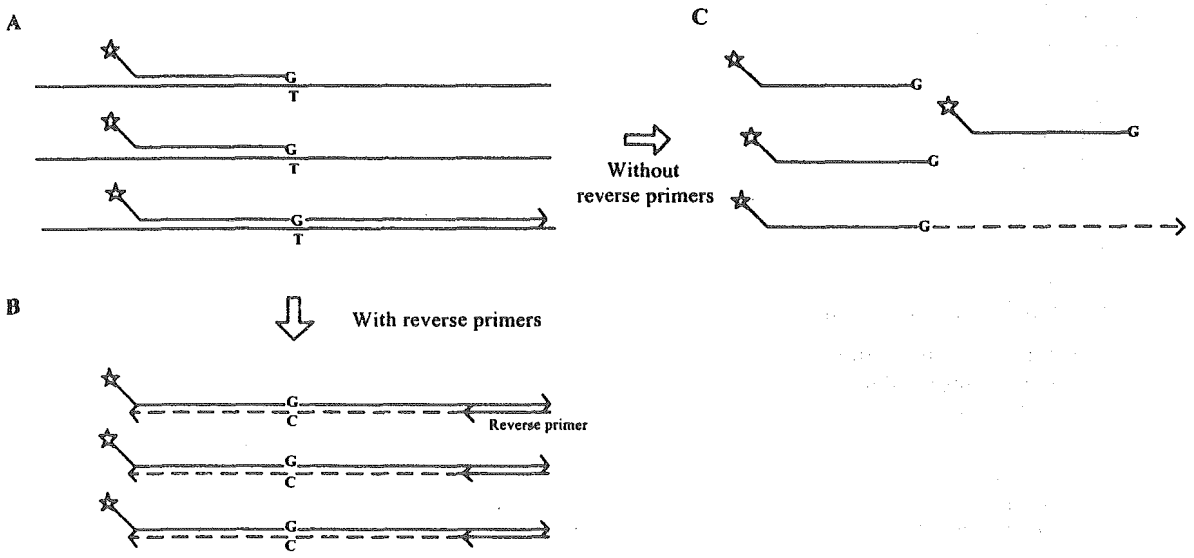

Fig. (1). Comparison between SSP-PCR and SSPCE.

Sequence-Specific Primers are designed with the 3'-terminus located at the SNP site and are elongated under optimal thermal cycling conditions (**A**). Mismatched primers may be elongated, and the elongated product would become a template for the reverse primers and would be amplified in SSP-PCR (**B**), but would not be amplified in SSPCE (**C**). Therefore, in SSP-PCR, non-specific amplification is the cause of amplification of error signals. In SSPCE, however, non-specific elongated primers are not amplified, and thus error signals are minimized.

[32]) and two genomic SNPs (FHC0134 : G → C at 10486 of exon 16 in MYH7 [33, 34] and FHC0153 : C → T at 12332 of exon 20 in MYH7 [35]), which are associated with hypertrophic cardiomyopathy. Each sequence-specific primer was designed to match the 3'-terminus at the SNP site and to adjust the melting temperature to around 60°C, as calculated by the Nearest Neighbor method [36]. Primers were labeled at the 5'-terminus with TAMRA or Cy5. The TAMRA-NHS ester was tagged via the NH_2-terminus of the oligonucleotide and phosphoamidite Cy5 was coupled using standard chemistry. All sequence specific primers were purified by HPLC in order to eliminate free dye. Synthesis, dye coupling and purification were performed by Sigma Genosys Japan. (Ishikari, Japan).

Amplification of the sequences containing SNP regions (1st PCR) was performed in a total volume of 20 μl including PCR reagents (Amplitaq Gold PCR Master Mix, Applied Biosystems, CA) and 5-10 ng of genomic DNA with the first 0.5 μM of the forward and reverse primers shown in Table 1. These primer sequences were designed to meet the general criteria of PCR and thermal cycling was performed as follows: 10 min at 95°C to activate Amplitaq Gold polymerase, followed by 40 cycles of 30 s at 95°C, 30 s at 58-70°C, 30 s at 72°C, and a final 2-10 min extension at 72°C.

SNP-specific elongation of sequence-specific primers (Table 1) was performed with the 5'-3' and 3'-5' exonuclease-free Stoffel Fragment of *Taq* polymerase (Applied Biosystems, CA) in 20 μl of reagents consisting of 1x Stoffel buffer (10 mM KCl, 10 mM Tris-HCl), 2.5 mM $MgCl_2$, 1 unit of Stoffel fragment, 20 nM of TAMRA- and Cy5-labeled primers and 1 μl of 1st PCR product.

The SSPCE sample containing elongated and non-elongated fluorescent-labeled primers was specifically measured by FCS. To fit the autocorrelation function ($G(t)$) of fluorescent fluctuation signals in a small confocal volume element to the theoretical model, the fraction and translational diffusion time of non-elongated primers (τ_1) and that of elongated primers (τ_2) in the SSPCE sample were determined as follows [37],

$$G(t)=\frac{1}{N}\left[\frac{y}{\left\{1+t/\tau_1\right\}\left\{1+s^2 t/\tau_1\right\}^{1/2}}+\frac{(1-y)}{\left\{1+t/\tau_2\right\}\left\{1+s^2 t/\tau_2\right\}^{1/2}}\right]$$

where y = fraction of non-elongated primers, (1–y) = fraction of elongated primers, τ = diffusion time of primer, τ_2 = diffusion time of elongated primer, N = number of molecules, $s = w_0/z_0$, where w_0 is the radius of confocal volume element and $2z_0$ is its length.

FCS measurements were conducted using an automated FCS measuring device (MF10S; Olympus Optical Co Ltd., Japan) equipped with two He-Ne Lasers emitting light at 543 nm (for excitation of TAMRA) and 633 nm (for excitation of Cy5). SSPCE reaction mixture (10 μl) was diluted 8-fold with 10 mM Tris buffer (pH 8.0) and measured in a 96-well glass bottom plate (Whatman Inc, NJ). The fraction of non-elongated (y) and elongated primers (1-y) were determined automatically with this device.

The Annealing temperature is important for SSPCE. Generally, wild-homo, mutant-homo and hetero DNA samples are used to determine the annealing temperature of each SNP. However, obtaining homo and hetero samples for each SNP is difficult, particularly with SNPs whose minor alleles have low frequency. Therefore, we constructed artificial control DNA for the major and minor samples. Artificial control DNA was made by using the primers containing the SNP site, as well as the reverse primers and products of the 1st PCR. One microliter of 1st PCR product of the pooled DNA (Novagen, Germany) was treated with Exonuclease I and alkaline shrimp phosphatase (Amersham Biosciences, UK) according to manufacturer's instructions in order to degrade excess primer and dNTPs. The sample was diluted 100-fold with 10 mM Tris Buffer (pH 8.0) and 1 μl of this solution was subject to PCR with 0.5 μM of primer, which included the SNP site located 3 bases from the 3'-terminus (Table 1), and 0.5 μM of the reverse primer used

Table 1. Primer Sequences for 1st PCR, Artificial Control DNA, and SSPCE

Mutation	1st PCR		Control DNA		SSP-Primer
G1958A	Forword	GGTCGAAGGTGGATTTAGCA	G Allele	TGGAAAGTGCACTTGGACGAA	GAAAGTGCACTTGGACG
	Reverse	TTCATCTTTCCCTTGCGGTA	A Allele	TGGAAAGTGCACTTGGACAAA	GAAAGTGCACTTGGACA
G12192A	Forword	ACATCATTACCGGGTTTTCCT	G Allele	TCTGACAACAGAGGCTTACGAC	TGACAACAGAGGCTTACG
	Reverse	AACATGGCTTTCTCAACTTT	A Allele	TCTGACAACAGAGGCTTACAAC	TGACAACAGAGGCTTACA
G15927A	Forword	TGAATCGGAGGACAACCAGT	G Allele	TAATACACCAGTCTTGTAAACCGGA	ATACACCAGTCTTGTAAACCG
	Reverse	TGGTACCCAAATCTGCTTCC	A Allele	TAATACACCAGTCTTGTAAACCAGA	ATACACCAGTCTTGTAAACCA
FHC0134	Forword	CTCCCTGATCCACTATGCC	C Allele	TTGTATCAGAAGTCTTCCCTCAACCT	GTATCAGAAGTCTTCCCTCAAC
	Reverse	GGTACAACCTGACATTGAAGTG	G Allele	TTGTATCAGAAGTCTTCCCTCAAGCT	GTATCAGAAGTCTTCCCTCAAG
FHC0153	Forword	CAGTGACAAAGCCAGGATCA	T Allele	CTATCAATGAACTGTCCCTCAAGG	CTATCAATGAACTGTCCCTCAA
	Reverse	GATCAATGTCCAGGGAGCTG	C Allele	CTATCAATGAACTGTCCCTCAGGG	CTATCAATGAACTGTCCCTCAG

in the 1st PCR. PCR was conducted with Amplitaq Gold polymerase mix in a total volume of 20 μl and touch down thermal cycling (95°C, 10 min for activation, followed by 40 cycles at 95°C (30 s), 70°C (30 s, -0.2°C per cycle), 72°C (30 s)).

The artificial control DNA was then used to estimate the annealing temperature for SSPCE to specifically elongate the primer at the target SNP. Fig. (2) shows the profiles of annealing temperature against elongation rate of the SSP primers with or without reverse primers. These profiles are typical of this method. For the mt1598 mutation, selective elongation is observed for a wide range of annealing temperatures with or without reverse primers. On the other hand, for the mt12192 mutation, there is short range of annealing temperatures with reverse primers. Without reverse primers, selective elongation is observed for a wide range of annealing temperatures. As mentioned before,

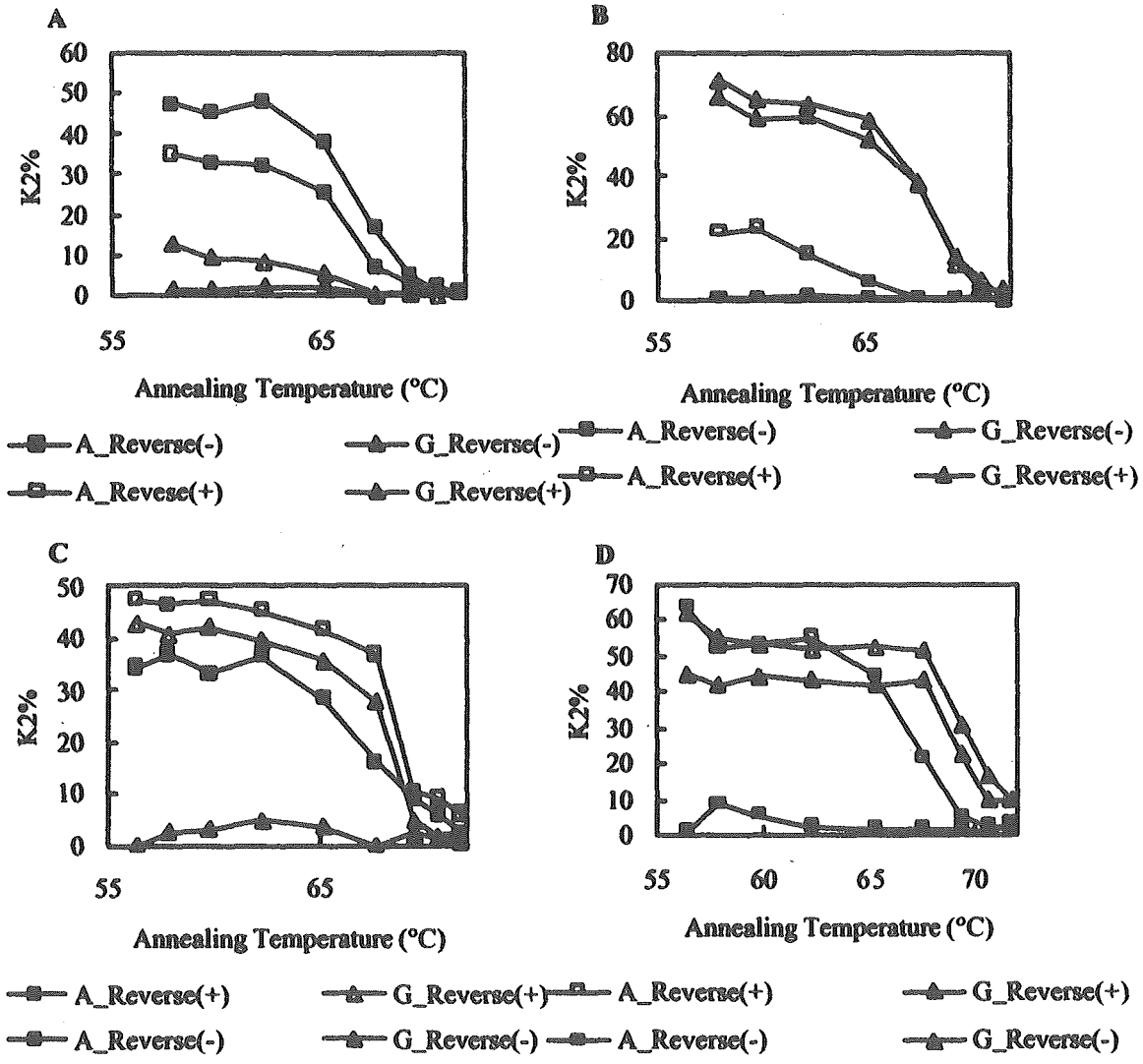

Fig. (2). The fraction of elongated SSP primers in SSP-PCR (with reverse primers) and SSPCE (without reverse primers) in relation to annealing temperatures.

Graph **A** shows the K2% (fraction of elongated primers) of A-specific primers to the A allele of mt1598 with reverse primers (A_Reverse (+)) or without reverse primers (A_reverse(-)), and to the G allele of mt1598 with reverse primers (G_Reverse(+)) or without reverse primers(G_Reverse(-)). Graph **B** shows the K2% of G-specific primers at mt1598. Graphs **C** and **D** show the K2% of A-specific and G-specific primers, respectively, at mt12192. In Graphs **A** and **B**, non-specific elongation is not observed in SSPCE (without reverse primer), while non-specific amplification is seen in SSP-PCR (with reverse primer) at lower annealing temperatures. Although it may be possible to determine the genotype of mt1598 by either method, there was a remarkable increase in non-specific amplification observed for mt12192. On the other hand, non-specific elongation was not observed with SSPCE in a wide range of annealing temperatures (**C**, **D**).

nonspecific elongation has only been discussed at the 3'-terminus. However, different profiles are seen for the same A/G transition mismatch in mt1598 and mt12192. In the case of mt12192, it appears to be difficult to optimize the conditions for SSP-PCR. Therefore, nonspecific amplification is related not only to the 3'-terminal base but also to the sequences around the SNP region. When compared with SSP-PCR, it is easier to optimize the conditions using the SSPCE method.

Fig. (3) shows the results for 9 samples, including both positive and negative samples. The cycle elongation profile was as follows: pre-denature, 95°C (2 min); 40 cycles at 95°C (30 s), 60-65°C (30 s), 72°C (30 s); and finally, elongation for 2 min at 72°C, annealing temperature was determined to be maximum K2% (fraction of elongated-primers) for specific elongation and minimum K2% for nonspecific elongation.

These 9 samples were sequenced using an ABI 3100 Genetic Analyzer (Applied Biosystems, CA) according to the manufacturer's instructions. All of the results were consistent with sequence data. The mitochondrial mutations presented in this paper were homoplastic. However, the mt1598 mutation was observed to be heteroplastic. Further experiments were conducted using these samples and the observed heteroplasmy may have been the result of sample preparation.

Fig. (4) summarizes the results for eighty samples subjected to SSPCE-FCS genotyping. The low rates of K2% in some samples were the result of poor amplification of the SNP region.

In the conventional SSP-PCR, some adjustments are required to determine the optimal conditions, and these conditions are determined by trial and error. Tested parameters include annealing temperature, Mg^{2+} concentration, primer concentration, and sequence of SSP primer (redesigning or changing the length). Particularly, for the mt12192 mutation mentioned above, substantial effort is required to determine optimal conditions. In contrast, the present SSPCE-FCS method requires only determination of the annealing temperature. It is laborious to investigate the influence of reagent concentration in PCR solution as well as that of annealing temperature. Recent commercially available thermal cyclers allow the annealing temperature to be readily determined. Therefore, it is advantageous for high-throughput SNP genotyping to be able to obtain optimal conditions simply based on the annealing temperature.

In the above method, 2 thermal cycling reactions are required; amplification of the SNP region (1st PCR), and

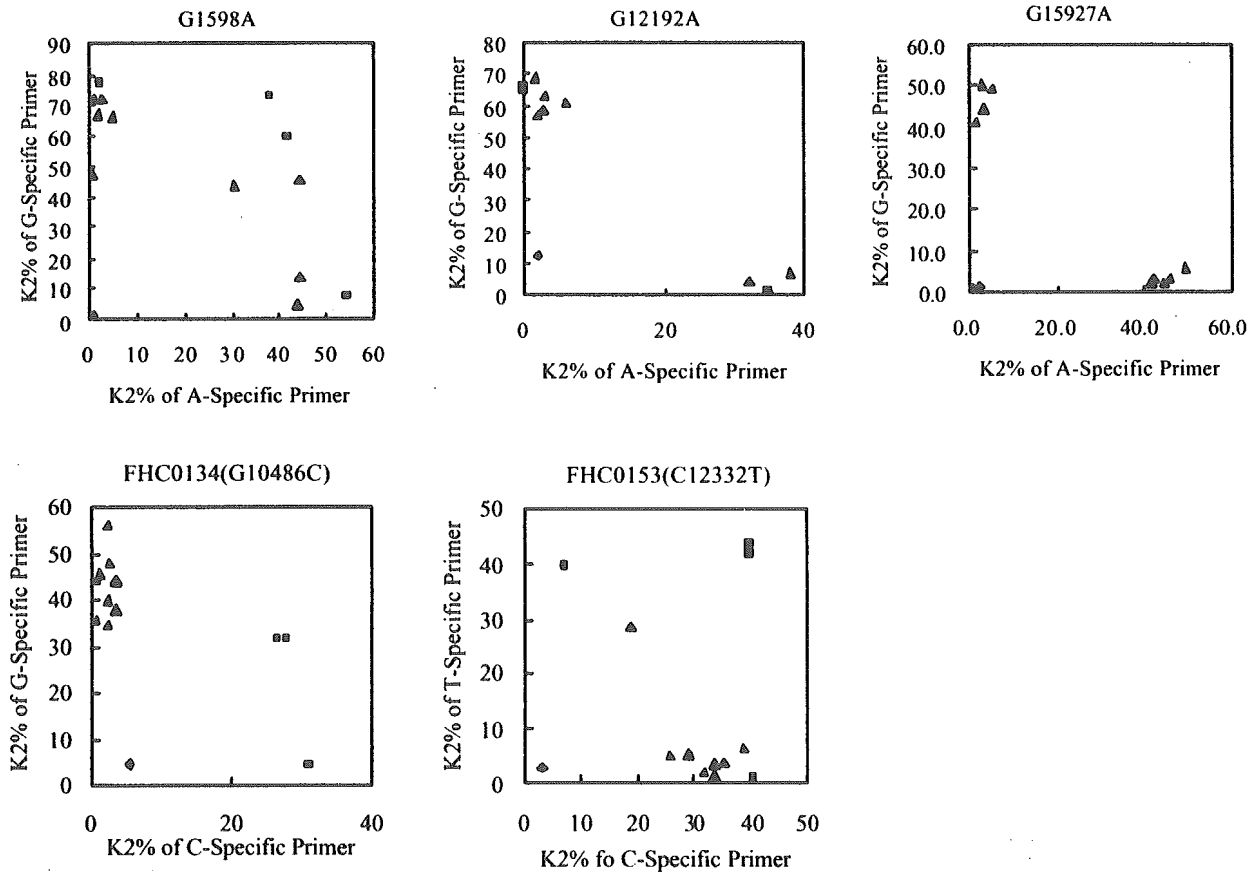

Fig. (3). Scatter plot of K2% for each SNP.

Each mutation is clearly typed for each of the 5 SNPs. In the Graphs, control and test samples are indicated as (■) and (▲), respectively. Each genotype was consistent with sequence data obtained using the ABI Prism 3100 Genetic Analyzer.

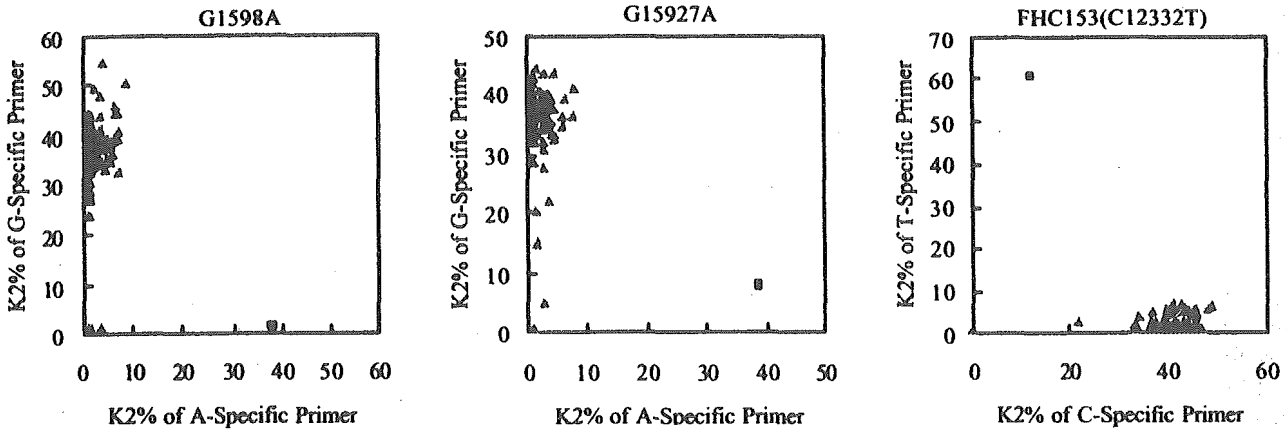

Fig. (4). Typing results in 80 samples for mt1598 mutation (G1598A), mt15927 mutation (G15927A), and FHC0153(C12332T).

Some samples exhibited low K2% in both alleles for each mutation. This was caused by failure of the 1st PCR. Alleles are clearly separated in the other samples. In the Graphs, control and test samples are indicated as (■) and (▲), respectively.

the SSPCE reaction. However, when analyzing numerous SNPs, substantial amounts of sample DNA are required when using conventional SSP-PCR. Because SSPCE-FCS needs only 1 μL of 1st PCR product, multiplexing the 1st PCR may considerably reduce the consumption of sample DNA. Furthermore, this method is simple and does not require separation or purification steps, thus making it very practical. Moreover, because tiny volumes of sample (less than 1 μL) are sufficient for FCS measurement, it may be possible to further reduce the PCR and SSPCE volumes to minimize consumption of reagents, thus minimizing expense.

CONCLUSION

There are numerous methods for high-throughput SNP genotyping. SSP-PCR is a very reliable method, provided that the optimal conditions are determined. However, this process is typically laborious. In contrast, SSPCE-FCS markedly simplifies the process, fully utilizing the discriminatory properties of DNA polymerase. This technique may open the way to high-throughput SNP genotyping using the principles of SSP-PCR.

ABBREVIATIONS

SSCP = Single Strand Conformation Polymorphism

SNP = Single Nucleotide Polymorphism

FCS = Fluorescence Correlation Spectroscopy

REFERENCE

[1] Brookes, A.J. (1999) *Gene*, **234**, 177-186.
[2] Elson, E. and Magde, D. (1974) *Biopolymers*, **13**, 1-27.
[3] Maiti, S., Haupts, U., Webb, W.W.(1997) *Proc. Natl. Acad. Sci. USA*, **94**, 11753-11757
[4] Eigen, M., Rigler, R. (1994) *Proc. Natl. Acad. Sci. USA*, **91**, 5740 – 5747.
[5] Björling, S., Kinjo,M., Földes-Papp, Z., Hagman, E., Thyberg, P., Rigler, R. (1998) *Biochemistry*, **37**, 12971-12978
[6] Walter, N.G., Schwille, P., Eigen, M. (1996) *Proc. Natl. Acad. Sci. USA*, **93**,12805-12810.
[7] Kinjo, M., Rigler, R. (1995) *Nucl. Acids Res.*, **23**, 1795-1799.
[8] Kinjo, M. (1998) *BioTechniques*, **25**, 706-715.
[9] Weber, S., Hummel, S.A., Weber, A.A., Zirwes, R.F., Weiner, O.H., Reuber, B.E. (2002) *Br. J. Haematol.*, **116**, 839-843.
[10] Huang, M.M., Arnheim, N., Goodman, M.F. (1992) *Nucl. Acids Res.*, **20**, 4567-4573.
[11] Kirk, B.W., Feinsod, M., Favis, R., Kliman, R.M., Barany, F. (2002) *Nucl. Acids Res.*, **30**, 3295-3311.
[12] Kwok, P-Y. (2001), *Annu. Rev. Genomics Hum. Genet.*, **2**, 235-258.
[13] Syvänen, A-C, *Nat. Rev. Genet.*, **2**, 930-942.
[14] Pease, A.C., Solas, D., Sullivan, E.J., Cronin, M.T., Holmes, C.P., Fodor, S.P.A. (1994) *Proc. Natl. Acad. Sci. USA*, **91**, 5022-5026.
[15] Griffin, T.J., Tang, W., Smith, L.M. (1997) *Nat. Biotechnol.*, **15**, 1368-1372.
[16] Ørum, H., Jakobsen, M.H., Koch, T., Vuust, J., Borre, M.B. (1999) *Clin. Chem.*, **45**, 1898-1905.
[17] Prince, J.A., Feuk, L., Howell, W.M., Jobs, M., Emahazion, T., Blennow, K., Brookes A.J. (2001) *Genome Res.*, **11**, 152-162.
[18] Livak, K.J. (1999) *Genet Anal.*, **14**, 143-149.
[19] Tyagi, S., Bratu, D.P., Kramer, F.R. (1998) *Nat. Biotechnol.*, **16**, 49-53.
[20] Barany, F. (1991) *Proc. Natl. Acad. Sci. USA*, **88**, 189-93.
[21] Baner, J., Nilsson, M., Mendel-Hartvig, M., Landegren, U. (1998) *Nucleic Acids Res.*, **26**, 5073-5078.
[22] Lyamichev, V. I., Kaiser, M. W., Lyamicheva, N. E., Vologodskii, A. V., Hall, J.G., Ma, W.P., Allawi, H.T., Neri, B.P. (2000) *Biochemistry*, **39**, 9523-9532.
[23] Buetow, K.H., Edmonson, M., MacDonald, R., Clifford, R., Yip, P., Kelley, J., Little D.P., Strausberg, R., Koester, H., Cantor, C.R., Braun, A. (2001) *Proc. Natl. Acad. Sci. USA*, **98**, 581-584.
[24] Chen,X., Levine,L. and Kwok,P-Y.,(1999) *Genome Res.*, **9**, 492-498.
[25] Alderborn, A., Kristofferson, A., Hammerling, U. (2000) *Genome Res.*, **10**, 1249-1258.
[26] Newton, C.R., Graham, A., Heptinstall, L.E., Powell, S.J., Summers, C., Kalsheker, N., Smith, J.C., Markham, A.F. (1989) *Nucleic Acids Res.*, **17**, 2503-2516.
[27] Gibson, N.J., Gillard, H.L., Whitcombe, D., Ferrie, R.M., Newton, C.R., Little, S. (1997) *Clin. Chem.*, **43**, 1336-1341.
[28] Thelwell, N., Millington, S., Solinas, A., Booth, J., Brown, T. (2000) *Nucleic Acids Res.*, **28**, 3752-3761
[29] Myakishev, M.V., Khripin, Y., Hu, S., Hamer, D.H. (2001) *Genome Res.*, **11**, 163-169.
[30] Obayashi, T., Hattori, K., Sugiyama, S., Tanaka, M., Tanaka, T., Itoyama, S., Deguchi, H., Kawamura, K., Koga, Y., Toshima, H., Takeda, N., Nagano, M., Ito, T. and Ozawa, T. (1992) *Am. Heart J.* **124**(5), 1263-1269.
[31] Shin, W.S., Tanaka, M., Suzuki, J., Hemmi, C. and Toyo-Oka, T. (2000) *Am. J. Hum. Genet.*, **67**, 1617-1620.